On the cause of the variation in tissue-maximum ratio values with source-to-detector distance

Bruce R. Thomadsen, Shrikant S. Kubsad, Bhudatt R. Paliwal, Siamak Shahabi, and T. Rockwell Mackie
Departments of Human Oncology and Medical Physics, University of Wisconsin—Madison, Madison, Wisconsin 53792

(Received 18 May 1992; accepted for publication 8 December 1992)

While tissue-maximum ratios (TMR) for ^{60}cobalt treatment units have been shown to be independent of source-to-axis distance (SAD), high-energy photon beams demonstrate variations in their TMR as a function of SAD. Some authors have asserted that the distance dependence of the TMR stems from electron contamination in the beams, while others have suggested low-energy, scattered photons as the cause. Using a magnet to sweep contaminant electrons out of the photon treatment beam eliminates any variation in TMR with distance. Thus, electron contamination accounts for all of the distance dependence, and any low-energy, scattered photons behave indistinguishably like the high-energy photons.

Key words: radiotherapy dosimetry, tissue-maximum ratio, tissue-phantom ratio, electron contamination, high-energy photon beams

I. INTRODUCTION AND BACKGROUND

Bagne[1] reported that the tissue-maximum ratio (TMR) for the 33- and 45-MV x-ray beams from a betatron exhibited a dependence on the source-to-detector distance, a characteristic not shown by lower-energy photon beams. Dawson[2] corroborated Bange's findings on a similar machine. Bagne suggested that the distance dependence stemmed from the difference in the relative amount of low-energy scattered photons (originating from interactions in the collimators) in the beam at various distances. Velkley *et al.*,[3] after noting a shift in the position of peak depth with source-to-skin distance (SSD) for a 25-MV betatron beam, suggested contaminant electrons as the cause, as Marinello and Dutreix[4] had previously for the shift in peak depth with field size. Similarly, Smith and Sutherland[5] also reported that the addition of 3 mm of acrylic reduced much of the shift in the depth of peak dose that accompanies varying the field size and SSD for a cobalt-60 unit. From this they also concluded that contamination electrons caused the shifts. Jayachandran[6] noted that with or without a 1.5-mm brass filter used to eliminate electron contamination from a cobalt-60 beam, the dose peaked at 3 mm, and that the brass filter made no appreciable change in the photon spectrum measured with a scintillation detector. Placing a 3-mm lead-equivalent glass in the beam markedly reduced the low-energy photon component of the spectrum, and shifted the peak depth to 5.5 mm, supporting the contention that low-energy scattered photons play some role in the shift of peak depth.

Marbach and Almond[7] made measurements with blocks screening a detector from the primary x rays in a 26-MV linear accelerator beam, and measured the transmission of the remaining scattered radiation through lead after filtering the beam through aluminum. Since the half-value layer of the resulting beam matched well that of the unblocked beam, they concluded that the shift in peak depth resulted from low-energy scattered photons, as suggested by Bagne.[1]

Dawson,[2] found that neither lead nor polystyrene attenuators of equal areal densities (kg/m^2) changed the distance dependence of the TMR. He concluded that electrons must be the cause, since the covers both affect electrons the same, while the lead would significantly reduce the dependence were it due to low-energy scattered photons (determined by Dawson[8] in a previous article to have an energy of about 200 keV for his 33-MV beam). Dawson found that contaminant electrons produced approximately 3% of the dose, even to depths of 5 cm.

Padikal and Deye[9] swept electrons out of a 10-MV photon beam with a magnet and found a sizeable (up to 18% for a 10×15-cm^2 field) contribution to the dose at the surface by the contamination electrons, but little (less than 1%) contribution at peak depth. Their conclusion was that contaminant electrons could not cause the shift in peak depth, so low-energy photons must be responsible.

Biggs and Ling[10] also used a magnet to sweep the electrons out of a 25-MV photon beam, and found that the field size dependence of the peak depth disappears. They concluded that the dependence stems from contaminant electrons. Biggs and Ling also repeated Marbach and Almond's experiment, but found that the transmission of the scattered radiation through lead as compared to that in polystyrene more closely followed the curve expected for electrons than photons. Biggs and Ling suggested that the aluminum screen used by Marbach and Almond may have initiated as many electrons as it stopped, giving them an unchanged beam.

Higgins *et al.*[11] investigated the contribution of contaminating secondary electrons to the skin dose from cobalt-60 beams. They found not only a component of electron contamination which fell rapidly in intensity with distance from the treatment unit head (due to electrons at the collimators or accessory tray), but also a component which

 0094-2405/93/030723-05$01.20

increased with distance, identified with electrons generated in the air between the source housing and the phantom or patient. Biggs and Russell[12] followed up on Biggs and Ling's 1979 work, investigating electron contamination with respect to distance for a wide range of beam energies from cobalt-60 to 25 MV. Biggs and Russell found that the intervening air column contributed a substantial part of the electron contamination. For the highest energy beam, they found that the component originating in the source head persisted to greater distances than that from lower-energy photon beams, and they suggested that such results are compatible with the conclusions of Petti *et al.*,[13] that the flattening filter and transmission dose monitors, rather than the collimators, generate most of the contaminant electrons in high-energy beams, so such electrons suffer less attenuation with distance at the patient (i.e., inverse-square law attenuation) than those arising from the collimators (i.e., originating closer to the patient). For lower-energy beams, the collimators appeared to contribute a higher fraction of the contaminant electrons. For the higher energy beams, Mackie[14] suggested that, in addition to less relative attenuation with distance, those electrons initiated in the forward direction (i.e., in the flattening filter) begin with the highest energies, and that the relatively higher energy electrons tend to scatter out of the beam less than lower energy electrons generated at greater angles in the collimators.

Mackie[14] also used a magnetic field to sweep contaminant electrons out of x-ray beams, and found that all differences in the TMR from the surface to the maximum disappeared for 6 and 15 MV.

While Biggs and Ling,[10] and Biggs and Russell[12] positively identified electron contamination in the higher-energy photon beams as the cause of the shift in peak depth with field size, and Mackie[14] demonstrated that electron contamination produces the differences in the TMR at shallow depths accompanying changes in source-to-phantom distance, the possibility still remained that the variations in TMR with distance at depths deeper than maximum may have both an electron and a low-energy photon component, as Johns and Rawlinson[15] have suggested. This current work addresses the question of whether contaminant electrons or low-energy, secondary photons cause the shift in peak depth and the differences in the TMR values after peak depth in a high-energy photon beam.

II. MATERIALS AND METHODS

This evaluation used the 24-MV photon beam from a linear accelerator (Varian Clinac 2500). As in the experiments of Padikal and Deye,[9] Biggs and Ling,[10] and Biggs and Russell,[12] initial measurements without a magnetic field across the beam record the detector's response to the photons and contaminant electrons. During subsequent measurements performed with a static magnetic field across the beam, only photon radiation exposed the detector. An unbiased, unshielded diode (Therados Corporation) served as the detector, with a similar diode, behind a constant thickness of build-up material, acting as a beam

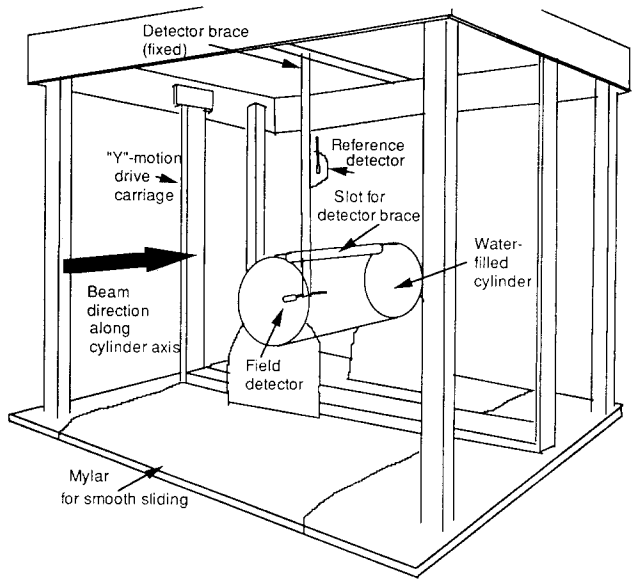

FIG. 1. Measurement apparatus. The detectors are fixed to a stationary holder. The "*Y*"-drive carriage moves the water-filled, cylindrical phantom along its axis, varying the thickness of the water in front of the detector.

reference. Both signals passed through the ratio circuitry of a scanning phantom system (RFA III, Therados Corporation), and the resulting ratio traced as the *y* input on an *x-y* plotter (Model 7044A, Hewlett–Packard). The selection of a diode as a detector was based on its spatial precision. While such an unshield diode yields depth dose curves for photon beams that differ from those measured by ionization chamber (due to increased sensitivity to lower-energy scattered photons), in this experiment any accentuated response becomes irrelevant because the photon component of the field remains the same with or without the magnetic field. An unshielded diode was selected so as not to remove any low-energy photon or electron contribution from the beam.

Figure 1 shows the measurement apparatus. A specially designed jig consisting of a Lucite arm held by a cross-bar attached to the scanning frame maintained the detector in a fixed location in space for each experimental run. The scanning frame, in turn, rested on an open, aluminum support, rather than in the usual plastic water tank. Around the diode, a 14-cm-diam water-filled acrylic tube provided the phantom material. Lucite braces at the ends held the tube's axis centered along the axis of the radiation beam, with the diode centered in the phantom. A slit along the top of the tube allowed the phantom to slide along the beam axis without interfering with the detector, to vary the thickness of material between the source and the detector. Attaching the front brace of the phantom to the "*Y*" scanning mechanism placed the position of the phantom, and thus the depth of the detector, under the control of the scanner. (In Therados's terminology, the "*Y*" direction corresponds to the direction requiring the movement of the entire cross-support mechanism.) Positioning the detector with its flat surface against the inner surface of the phan-

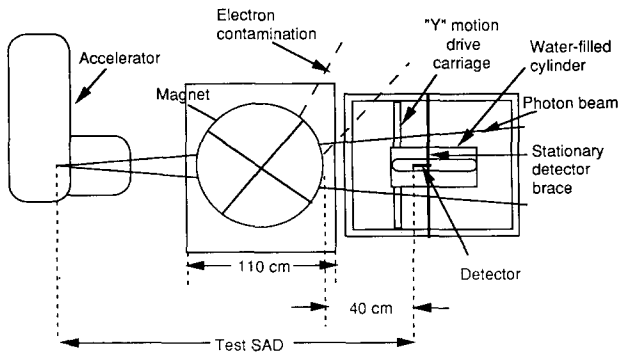

FIG. 2. Measurement setup. When energized the magnet sweeps the electron contamination component out of the accelerator's 24-MV x-ray beam.

tom placed the detector at its minimum depth of 2 mm. The "*Y*" position signal provided the *x* input for the *x*-*y* plotter. For analysis, the curves were digitized into a computer (Altek digitizing table, Model AL30; Digital Equipment Corporation micro VAX-II).

In all cases the collimated photon beam's edges fell outside of the phantom, so at any given depth, the boundary of the phantom limited the amount of phantom-generated scatter, holding the phantom scatter constant, and independent of collimator opening.

Figure 2 illustrates schematically the experimental setup. The beam from the accelerator passed between the poles of a large magnet before falling on the detector system. The magnet's width of 110 cm restricted the minimum source-to-detector distance (SDD) to 205.5 cm. In addition to that distance, measurements were also performed at source-to-detector distances of 314 and 404 cm, in each case using collimator settings which would produce field sizes projected at 100 cm from the source of 10×10 cm^2, 20×20 cm^2, and 35×35 cm^2. In all cases, the distance from the end of the magnet's poles to the detector remained constant (40 cm) to avoid differing amounts of electron contamination produced in the column of air between the magnet and the detector. The 101.5-cm aperture allowed passage of the beams without direct contact with the magnetic poles or support, except for the 35×35-cm^2 beam edge at the longest SDD. Even in this large field situation, any scatter or contamination generated in the magnetic poles contributes negligibly to the resultant curves. (See Figs. 3 and 4.)

For each combination of collimator setting and SDD, scans were recorded without and with the presence of a magnetic field. A 0.04-T magnetic field removed all of the electrons from a 22-MeV electron test beam, leaving only the bremsstrahlung component. Petti *et al.*,[13] using Monte Carlo techniques, calculated that all of the contaminating electrons for the 25-MV photon beam from a Varian Clinac-35 have energies below 19 MeV. The actual experimental runs used magnetic fields of 0.4 Tesla, a factor of 10 over the field strength at which the traces for the 22-MeV electron beam stopped showing any electron component. Measurements of the magnetic field strength used two independent systems (Rawson Rotating Probe, type 501, and an Empire Hall Probe, model 900), as described by Wessels *et al.*[16]

III. RESULTS

Figure 3(a), (b), and (c) each show the traces for one of the three collimator settings. Each figure depicts the traces for the three distances without the magnetic field (solid lines) and with the magnetic field (dashed or dotted lines). The normalization for all of the curves at a 15-cm depth falls well beyond the deepest reach of any electron contamination.

The shift in peak depth and the differences in the "tissue-phantom ratio" (TPR) at shallower depths show clearly for the beams in the absence of the magnetic field. (Such a normalization would make the curves tissue-phantom ratios were the phantom larger than the field. Not strictly following the definition, the term as used in this experiment falls within quotation marks to note the difference.) However, with the magnetic field, both the peak depth shift and the differences in the TPR disappear, to within the uncertainty of the experiment.

In addition to investigating the variations of TPR with distance, correlation of the experimental results by collimator setting for a given distance corroborated the results of Biggs and Ling,[10] Biggs and Russell,[12] and Mackie,[14] that contamination electrons alone accounted for the observed differences in peak depths and shallow-depth TPR values which accompany field size changes with high-energy photon beams (see Fig. 4).

The small "vibrations" in the computer-plotted curves reflect the small variation in the signal intensity.

IV. DISCUSSION

The results of this experiment indicate that, for this high-energy photon beam, both the shift in the depth of peak dose with SAD and the variations in shallow-depth TPR with SAD stem from the same cause: contaminating secondary electrons. Any "lower-energy" photon component appears to behave in a manner indistinguishable from the primary beam. Narrow beams tend to be "self-cleaning" of contamination (Attix *et al.*[17]), because electrons scatter out of the field ("out-scatter") through interactions with the medium. In large fields, on the other hand, scatter towards the center of the field ("in-scatter") balances the out-scatter. Thus, the effects of contamination appear more prominent with larger field sizes. The table gives the maximum amount of electron scatter, as a fraction of the x-ray peak dose, for each of the combinations of

TABLE I. Percent of peak dose contributed by electron contamination.

Collimator setting (Field size at 100 cm) [cm2]	Source detector distance (cm) 205.5	315	404
10×10	0.4	1.5	2
20×20	5.3	4.2	5
35×35	10.2	6.6	7.5

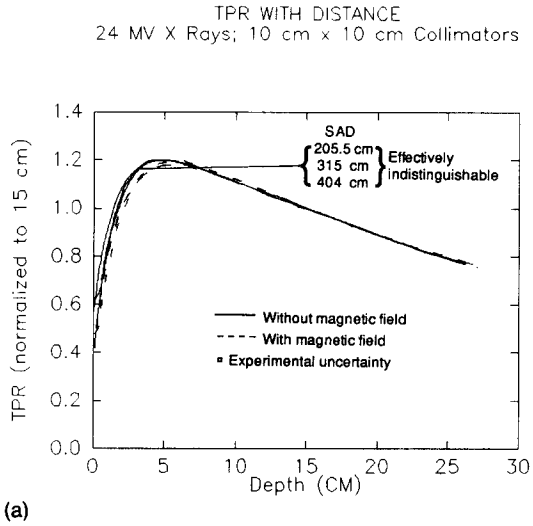

FIG. 3. Measured tissue-phantom ratios (TPR) vs depth as a function at source-to-detector distance. For each of the collimator settings, TPR curves were measured at three source-to-detector distances, with and without an applied magnetic field across the beam. The square labeled "Experimental Uncertainty" illustrates the approximate size of two standard deviations for both variables: (a) 10×10-cm collimator setting, (b) 20×20 cm-collimator setting, and (c) 35×35-cm collimator setting.

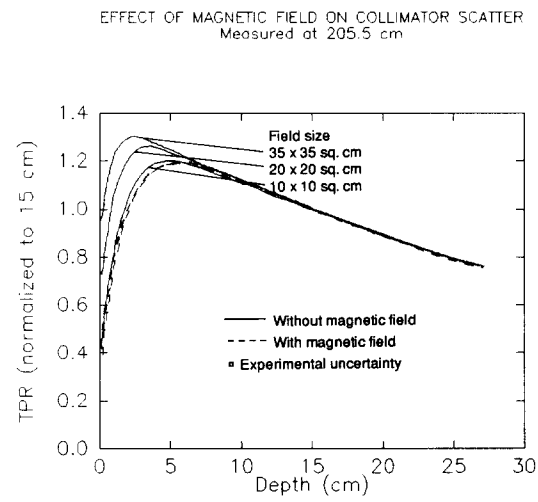

FIG. 4. Measured tissue phantom ratios vs depth as a function of collimator setting for 205.5-cm source-to-detector distance, with and without an applied magnetic field in the beam.

field size and SDD. The shortest SAD used in this experiment (205.5 cm) is twice the normal SAD (100 cm), which exhibits a distance dependence of about the same amount as at 100 cm. Were there any low-energy photon component contributing to the distance dependence at 100-cm SAD, some would still persist at 205.5 cm.

For a given collimator setting, after 5 cm, the TPR for each of the different distances superimpose, even without the magnetic field. This follows the results of Johns *et al.*[18] who demonstrated the invariance of TAR with distance for a cobalt-60 beam. With the cobalt-60 beam, the contaminating electrons fail to penetrate either the build-up cap used for "in-air" measurements, or to the peak depth of 0.5 cm with in-phantom measurement, making the contamination electrons "invisible" in such measurements. That Bagne[1] and Dawson[2] for various SAD found different values of TMR well beyond the range of the most energetic electron contamination probably resulted from varying amounts of electron contamination being included in the normalizing "maximum" measurement as the source of phantom distance varied. Such an effect would not be seen with the TPR normalized at 15 cm.

It appears that, for a small collimator setting, the air column between the source housing and the phantom contributes an increasing fraction of the contaminant electrons as the distance increases, although probably following something like a build-up function. For large field sizes, the source housing (collimators, flattening filter, etc.) contributes a much larger portion of the contamination. This component decreases relatively quickly with distance (due to inverse-square attenuation), and is replaced only partially by contamination from the increasing volume of air accompanying increased distance. For the middle-range field size, over the range of distances measured, the two processes compete in such a manner as to give a fairly constant contamination with changes in distance. These findings agree with results of Biggs and Russell.[12]

The electron component of the treatment beams complicates performing accurate dosimetry, dictating the use of different tables for each significantly different target distance used clinically. The complications increase when using TMR (as stated above) which includes the contamination in the normalization. While relegating the problem to shallow depths, the use of TPR fails to eliminate dosimetry problems because of the difficulty in separating the effects of collimator-setting-related variations in the amount of radiation incident on a patient from the patient-generated scatter contribution to the dose at a point. The best solution to the problem seems to lie in the development of a "cleaning" magnet which could fit under the shielding-block tray on an accelerator's source housing. Such a magnet could then sweep those electrons produced in the source head out of the beam. This would still not produce beams as "clean" as those in this experiment for the longer source-to-patient distances, because of the increased column of air which would be encountered clinically. However, if the magnet could be supported on an extension arm, and moved to a preset distance from the patient, consistent and invariant beams could be produced.

V. CONCLUSIONS

For a 24-MV x-ray beam from a linear accelerator, the variations in the peak depth and the shallow-depth values of the tissue-phantom ratio observed with changes in source-to-detector distances originate solely from secondary electron contamination in the photon beam.

ACKNOWLEDGMENTS

The completion of this work relied upon the significant contributions of Darrell Loper, Peter van de Geijn, Mark Gehring, and particularly Jan van de Geijn, who first introduced the use of the cylindrical water phantoms into our department in 1977.

[1]F. Bagne, "Physical aspects of supervoltage x-ray therapy," Med. Phys. **1**, 266–274 (1974).

[2]D. J. Dawson, "Tissue-maximum ratios for high-energy x-rays," Med. Phys. **4**, 423–430 (1977).

[3]D. E. Velkley, D. J. Manson, J. A. Purdy, and G. D. Oliver, Jr., "Build-up region of megavoltage photon radiation source," Med. Phys. **2**, 14–19 (1975).

[4]G. Marinello and A. Dutreix, "Etude Dosimetrique d'un Faisdeau de Rayons X de 25 MV," J. Radiol. Electrik. **54**, 951–958 (1973).

[5]C. W. Smith and W. H. Sutherland, "Electron contamination of telecobalt beams," Br. J. Radiol. **49**, 562–563 (1976).

[6]C. A. Jayachandran, "Gamma-ray scatter in a telecobalt beam," Br. J. Radiol. **49**, 563–564 (1976).

[7]J. R. Marbach and P. R. Almond, "Scattered photons as the cause for the observed d_{max} shift with field size in high-energy photon beams," Med. Phys. **4**, 310–314 (1977).

[8]D. J. Dawson, "Percentage depth dose for high energy x-rays," Phys. Med. Biol. **21**, 226–235 (1976).

[9]T. N. Padikal and J. A. Deye, "Electron contamination of a high-energy x-ray beam," Phys. Med. Biol. **23**, 1086–1092 (1978).

[10]P. J. Biggs and C. Ling, "Electrons as the cause of the observed d_{max} shift with field size in high energy photon beams," Med. Phys. **6**, 291–295 (1979).

[11]P. D. Higgins, C. H. Sibata, F. H. Attix, and B. R. Paliwal, "Calculational methods for estimating skin dose from electrons in Co-60 gamma-ray beams," Med. Phys. **10**, 622–627 (1983).

[12]P. J. Biggs and M. D. Russell, "An investigation into the presence of secondary electrons in megavoltage photon beams," Phys. Med. Biol. **28**, 1033–1043 (1983).

[13]P. L. Petti, M. S. Goodman, J. M. Sisterson, P. J. Biggs, T. A. Gabriel, and R. Mohan, "Sources of electron contamination for the Clinac-35 25-MV photon beam," Med. Phys. **10**, 856–861 (1983).

[14]T. R. Mackie, "A Study of Charged Particles and Scattered Photons in Megavoltage X-Ray Beams," thesis, University of Alberta (1984).

[15]H. E. Johns and J. A. Rawlinson, "Desirable characteristics of high energy photon and electrons," in *High Energy Photons and Electrons,* edited by S. Kramer, N. Suntharalingam, and G. F. Zinninger (Wiley, New York, 1976), p. 11.

[16]B. W. Wessels, B. R. Paliwal, M. J. Parrott, and M. C. Choi, "Characterization of Clinac-18 electron-beam energy using a magnetic analysis method," Med. Phys. **6**, 45–48 (1979).

[17]F. H. Attix, F. Lopez, S. Owolabi, and B. R. Paliwal, "Electron contamination in Co-60 gamma-ray beams," Med. Phys. **10**, 301–306 (1983).

[18]J. E. Johns, G. F. Whitmore, T. A. Watson, and F. H. Umberg, "A system of dosimetry for rotation therapy and typical rotation distributions," J. Can. Assoc. Radiol. **4**, 1–14 (1953).